CHEMICAL ENGINEERING TRANSACTIONS
VOL. 36, 2014
A publication of AIDIC
The Italian Association of Chemical Engineering
www.aidic.it/cet
Guest Editors: Valerio Cozzani, Eddy de Rademaeker

ISBN 978-88-95608-27-3; **ISSN** 2283-9216
DOI: 10.3303/CET1436062

Experimental and Numerical Characterization of Fireproofing Materials Based on ASTM E162 Standard

Francesca Argenti[a], Ludovica Guerrini[b], Francesco Rossi[c], Gabriele Landucci[a]*

[a] Dipartimento di Ingegneria Civile e Industriale - Università di Pisa Largo Lucio Lazzarino 1, 56126, Pisa, Italy
[b] Dipartimento di Ingegneria Industriale (DII) – Università di Padova. Via Marzolo 9, Padova, Italy.
[c] Consorzio Polo Tecnologico Magona, Via Magona, 57023, Cecina (LI), Italy.
g.landucci@diccism.unipi.it

Fires may affect process and storage equipment causing severe damages and potential accident escalation. Passive protections, based on the application of fireproofing coatings, are usually implemented in order to prevent or mitigate such events. The design and testing of this type of barriers is a critical task due to the extreme heat exposure conditions. For this purpose, several standard tests, based on the use of large scale furnaces and experimental facilities, are adopted.
In the present study, a methodology for the assessment of fireproofing materials performance was presented. The methodology was aimed at reducing the costs of fire tests by the combined use of small scale experiments and modeling activities. A novel inorganic formulation based on basalt fibers and silica aerogel was tested and compared with commercial fireproofing materials. A specific Key Performance Indicator (KPI) was evaluated in order to support the effective design of passive fire protections.

1. Introduction

Severe fires may affect process equipment or transport vessels leading to a catastrophic loss of containment (Roberts et al., 2000). The adoption of passive fire protection materials (PFP), e.g. installation of protective coatings able to withstand severe fire exposure conditions, represents an effective solution for the protection of fired equipment structures (Tugnoli et al., 2013) and a highly safe strategy for risk reduction (Tugnoli et al., 2012) and lay-out definition in oil and gas industries (Di Padova et al., 2011). Several standards rule the specific design and testing of PFP materials (UL 1709, ASTM E 119, ASTM E 1529, OTI 95635, and ISO 22899-1, among others), demonstrating the importance of PFP testing in severe heat exposure conditions, thus reproducing real scale fires, in order to evaluate the actual PFP protection performance. Consequently, several experimental configurations on large (Townsend et al., 1974) or pilot scale have been proposed (Birk et al., 2006). The main advantage of such large scale tests is that design guidelines for PFP systems can be directly derived for the application on industrial equipment, without requiring scale up protocols (Droste and Schoen, 1988). On the other hand, large scale tests are not easily reproducible and require high financial efforts for experimental set up preparation and management. In addition, their realization may arise environmental and safety concerns. Therefore, in order to carry out a preliminary design and screening of novel or consolidated PFP materials or formulations, laboratory (Gomez-Mares et al. 2012a) and bench scale (Landucci et al., 2009a) tests are an effective solution, with lower costs both for equipment and tested specimens.
In the present work, a methodology for the assessment of fireproofing performance was developed. The methodology, based on combined experimental and modeling activities, was aimed at the characterization and development of innovative inorganic fireproofing materials based on the combined use of silica aerogel and basalt fibers tissue. Experimental characterization of materials behaviour was performed through a small scale fire test, based on the ASTM E162 standard (ASTM, 1994). Then, a simplified model was developed to reproduce test conditions and to extend the analysis to fire exposure conditions and durations relevant for real scale applications. Finally, PFP performances of the novel materials were assessed and compared against other inorganic formulations.

Please cite this article as: Argenti F., Guerrini L., Rossi F., Landucci G., 2014, Experimental and numerical characterization of fireproofing materials based on astm e162 standard, Chemical Engineering Transactions, 36, 367-372 DOI: 10.3303/CET1436062

2. Materials and methods

2.1 Experimental characterization of PFP materials

The tested PFP products were innovative manufactured products realized by enclosing one or more layers of a silica aerogel into a thin basalt fiber tissue blanket. The basalt fiber tissue adopted as external covering was Fabric Type BAS 630.1270.T, provided by Basaltex. The selected silica aerogel, constituted by light weight silica solids (void fraction of 97%), was Pyrogel XTF provided by Aspen Aerogels. In order to reproduce fire exposure conditions on a piece of equipment or pipe, thus monitoring the response of the protected target, each tested insulating coating was coupled with a 5mm thick low carbon steel board obtaining a test specimen. The main geometrical features of the tested specimens are reported in Table 1.

Table 1: Conditions and specimen features during considered in the fire tests

Test ID	Radiant Panel Temperature (°C)	Number of aerogel layers	Nominal aerogel thickness (mm)	Measured aerogel thickness (mm)
T1	740	1	10	10
T2	740	4	40	35

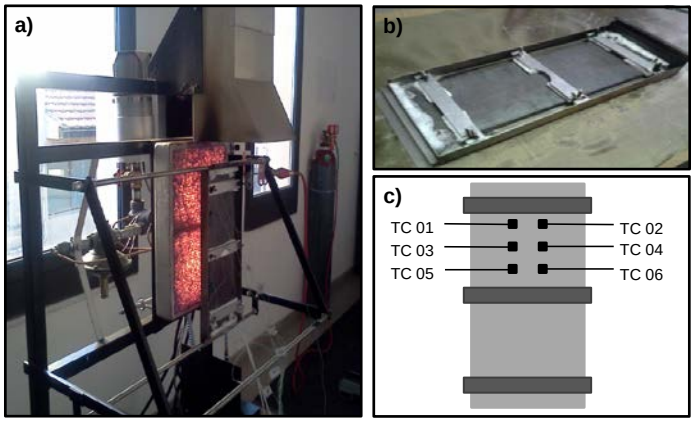

Figure 1: Small scale fire test facility: a) overview b) detail of the specimen support c) scheme of thermocouples positioning.

Figure 1a) shows the overview of the experimental facility. The whole set-up, namely RP-1A model, was supplied and certified by Govmark Inc for testing materials according to the standard ASTM E 162 (ASTM, 1994). The framework consisted of the supporting structure made of stainless steel covered by epoxy varnish. The support frame (see detail b) of Figure 1), made of aluminum, was fixed to the main framework in order to hold material samples with dimensions in accordance with (ASTM, 1994), e.g. 150 x 460 mm and variable thickness. The radiating panel, featuring a radiating surface of 300 x 460 mm, is made of porous refractory material and was vertically mounted on a stainless steel framework. The modifications introduced in the standard set up basically concerned the orientation of the specimen, which was set parallel to the radiating panel. Shortening the separating distance between the specimen and the radiating panel allowed increasing the severity of the heat exposure. Besides, the selection of LPG instead of methane as fuel gas also increased the thermal potentiality of the apparatus, which could provide heat radiation in the range 10÷50 kW/m^2. The flame generation system consisted of the fuel gas pressurized cylinder and the supplying system connected to the flame generator. On the fuel line, appropriate devices allowed pressure and flow regulation. In the tests, the LPG flow was set to 10 L/s, while air flow was set to 50 L/s. The panel was equipped with a Venturi fan for fuel gas and air mixing.

Each experimental trial was carried out for 40 minutes. During the test, the temperature of the steel board was measured by six Chromel-Alumel type K thermocouples positioned at the interface between the coating layer and the protected steel board. Thermocouples position is shown in Figure 1 c). Hence, dynamic temperature profiles were derived from every experimental run to characterize the performances of PFPs.

2.2 Numerical modelling of PFP materials performances

In the second phase of the study, the experimental results were analyzed, integrated and extended through a numerical approach, based on the implementation of a simplified model aimed at reproducing the average temperature profile in the specimen exposed to fire.

A one-dimensional model was developed assuming that, during the test, the heat propagation through the sample exposed to radiant heat takes place mainly in the direction perpendicular to the exposed face. Therefore, the occurring heat exchange phenomena were described by a system of Partial Differential Equations for transient one-dimensional thermal conduction in the adjacent layers of different material. In order to consider the thermal conductivity of coating material as variable with temperature, the above described system was solved through numerical integration by adopting a spatial discretization in the direction of thickness, in accordance with the "thermal nodes modeling" approach (Modest, 2003). A non-uniform mesh designed to be finer in the proximity of the interface between different layers and a time step of one second were selected. A pure radiative model was adopted: Stefan-Boltzmann's law was applied to calculate the total heat flux received by the specimen, considering the radiating panel as a black body (emissivity equal to 1) and a constant value of "effective radiant temperature" was selected to account for the convective heat transfer contribution of hot gases flowing over the exposed surface of the specimen.

The equations implemented in the model are reported in Table 2 together with the initial and boundary conditions required for solution, while Table 3 summarizes the adopted nomenclature.

Table 2: Transient heat balance equations implemented in the one-dimensional model

ID	Equation	Description
1	$\rho_{ins} \cdot cp_{ins} \cdot \frac{\partial T}{\partial t} = \frac{\partial}{\partial x}\left(k_{ins} \cdot \frac{\partial T}{\partial x} \right)$	Heat balance equation for the aerogel layer
2	$\frac{\partial T}{\partial t} = \alpha_{basalt} \cdot \frac{\partial^2 T}{\partial x^2}$	Heat balance equation for the basalt fiber layer
3	$\frac{\partial T}{\partial t} = \alpha_{s} \cdot \frac{\partial^2 T}{\partial x^2}$	Heat balance equation for the steel board
4	$k_{basalt} \cdot \left.\frac{\partial T}{\partial x}\right\|_{\substack{exposed \\ side}} = \sigma_B \cdot \left(\varepsilon_{rad} \cdot T_{rad}^4 - \varepsilon_{ins} \cdot T_{ins}^4 \right)$	Boundary condition 1: front side exposed to radiant panel
5	$k_s \cdot \left.\frac{\partial T}{\partial x}\right\|_{\substack{rear \\ side}} = h_{air} \cdot \left(T - T_{air} \right)$	Boundary condition 2: rear side of the steel board
6	$k_{basalt} \cdot \left.\frac{\partial T}{\partial x}\right\|_{\text{int erface}} = k_{ins} \cdot \left.\frac{\partial T}{\partial x}\right\|_{\text{int erface}}$ $k_{basalt} \cdot \left.\frac{\partial T}{\partial x}\right\|_{\text{int erface}} = k_{i} \cdot \left.\frac{\partial T}{\partial x}\right\|_{\text{int erface}}$	Boundary condition 3: continuity of heat flux at layer interface
7	$T_{basalt}(t) = T_{ins}(t)$ $T_{basalt}(t) = T_{s}(t)$	Boundary condition 4:continuity of temperature at layer interface
	$T_{basalt}(t=0) = T_{ins}(t=0) = T_{S}(t=0) = T_{air}$	Initial condition: uniform temperature in all layers

A variable value with temperature was considered for k_{ins}; an average constant value was considered for α_{basalt} and α_s.

Table 3: Nomenclature adopted in the present study

Item	Definition	Subscript	Definition
cp	Heat capacity	air	Air
k	Thermal conductivity	basalt	Basalt fiber tissue
x	Spatial coordinates in thickness direction	ins	Aerogel layer
t	Time	rad	Radiating panel
T	Temperature	s	Steel
α	Thermal diffusivity		
ε	emissivity		
ρ	Density		
σ_B	Stefan Boltzmann's constant		

The thermo-physical properties of PFP materials were given as input data to the model. Constant average values were adopted to describe the behavior of the steel and the basalt fiber tissue. The aerogel density and heat capacity were derived from the manufacturer data sheet, while the thermal conductivity was

calculated as a function of temperature by means of a correlation derived applying a fitting procedure to effective thermal conductivity data measured by Wei et al. (2011).
The adoption of an effective thermal conductivity derived from experimental data was necessary to avoid the use of complex models describing all concurrent phenomena at microstructural level that govern heat transfer within highly porous materials (Gomez-Mares et al., 2012b).

3. Results and discussion

3.1 Experimental results and model validation

Figure 2 reports the experimental results obtained with the modified ASTM E 162 set up. In particular, the dynamic temperature behavior of the tested specimen recorded by the thermocouples is reported in Figure 2a and 2b for test T.1 and T.2 respectively (see Table 1). As shown in Figure 2, the measured temperatures were characterized by an increasing trend moving from the bottom to the top of the specimen, i.e. the higher temperature value was registered by thermocouple TC 02, while the lower temperature value were registered by thermocouple TC 06 (see Figure 1c for thermocouples positioning). The same behavior was also evidenced in leftmost side of the board. This phenomenon was due to the convective contribution to heat transfer by buoyant hot gases flowing upwards in the free space between the radiant panel and the exposed face of the specimen. The results confirmed that increasing the thickness of the aerogel layer allowed for an improvement of the protective performance. In fact, the average predicted temperature was reduced from 234 to 165°C after 40 minutes of heat exposure (end of the test).

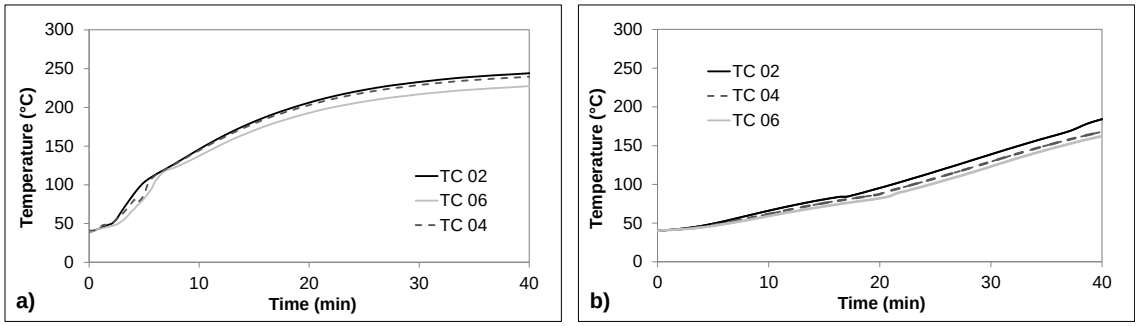

Figure 2: Experimental results: measured dynamic temperatures of the protected steel board for test T.1 (a) and T.2 (b).

The experimental results were used for the validation of the model described in Section 2.2. Figure 3 shows validation results for test T.1 (Figure 3a) and test T.2 (Figure 3b) respectively. As shown in the figure, despite the strong simplifications introduced in the model (e.g., one-dimensional heat propagation, average density and heat capacity) the agreement with predicted and measured temperatures was quite good, allowing the model application for data extrapolation for prolonged heat exposure and to higher heat radiation values.

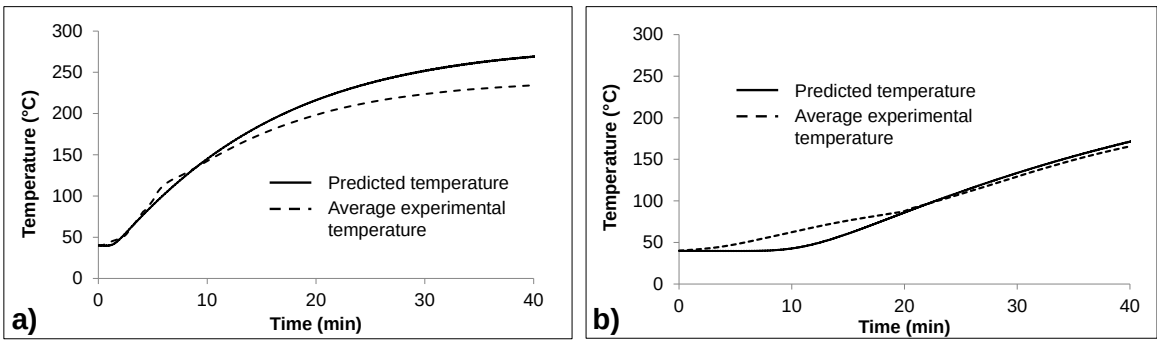

Figure 3: Model validation against experimental results: a) 1 layer of aerogel b) 4 layers of aerogel.

3.2 Performance assessment of PFP materials

Once validated, the model was applied for extrapolating the behavior of the protected steelwork in presence of large scale fires, e.g. higher heat radiation values, and different fireproofing configurations. In particular, the engulfment in a hydrocarbon pool fire was simulated considering a radiation source at 1098°C, which is the maximum radiant temperature reached during UL 1709 standard test, and an extended fire exposure time of 100 minutes was considered.

The key performance indicator TI (temperature index) suggested by Landucci et al. (2009b), was calculated for each simulated coating type and thickness. In this work, TI was defined as the ratio between the maximum temperature reached by the non-exposed surface of the steel board and the temperature of the external coating surface, as derived from simulation results. The normalized index was suitable to provide an effective and rapid estimation of the temperature gradient within the specimen thickness and, hence, of the thermal insulation capability of the analyzed coating material.

Figure 4a shows the temperature profiles predicted by model simulations for products made up of one, two and four internal layers of aerogel respectively. The predicted profiles for specimen coated with silica blanket (nominal thickness of 20 and 40 mm) were also reported for comparison. Silica blanket properties were modeled according to the values suggested in a previous work (Argenti and Landucci, 2013); the compression effects on thermal conductivity were also taken into account, following the previously described approach. Silica blanket represented a suitable benchmark since it is an inorganic fireproofing solution prescribed for application on pressurized fixed equipment as well as road and rail tankers (Birk, 2005). The illustrated results highlighted that, for a given thickness, the innovative fireproofing product showed worse insulation properties respect to silica blanket. Nevertheless, similar temperature behaviors were predicted comparing 4 layers of aerogel respect to 20mm of silica blanket.

Figure 4b reports the maximum values of the performance index TI (reached at the end of simulation runs) for all defined case studies. The horizontal line represents the threshold value of TI (namely TI* = 0.36), calculated as the ratio between the reference temperature value for the thermal weakening of the steel, fixed at 400 °C according to references in the literature (Cotgreave, 1992), and the standard hydrocarbon fire temperature (e.g., 1098°C) (UL 1709 standard test).

Figure 4b shows that for the fireproofing material tested in the present study, the TI index reached values above TI* in all the simulated cases. Nevertheless, only in the case of one or two layers of aerogel the predicted values is significantly above the TI* threshold, with potentially critical conditions for the structural integrity of the protected steelwork due to insufficient insulation performances.

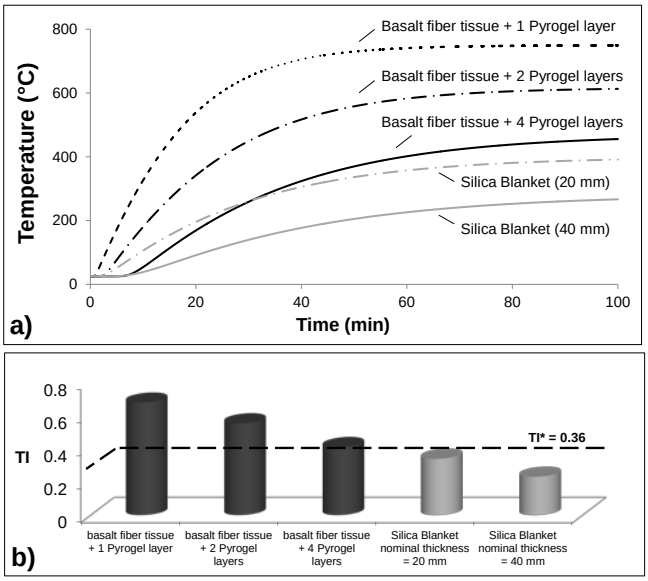

Figure4: Model application to simulate severe fire exposure conditions for different PFP configurations: a) temperature vs time prediction; b) TI index evaluated at the end of the simulation.

Even if the simplified model did not take into account some aspects which affect vessels resistance to fires, which would require advanced modeling (Venart, 1999) (e.g., increasing vessel pressure due to heat load, inner fluid behavior, etc.), the simulation results allowed identifying the safety margins available for

thermal protection design. Therefore, the simplified model was demonstrated to be a simple tool for the preliminary screening and assessment of PFP performances.

4. Conclusions

An integrated experimental and numerical approach for the assessment of inorganic PFP materials performances was presented. A novel inorganic formulation, based on silica aerogel and basalt fibers was tested in order to exemplify the methodology. The experimental set up, derived from a modified ASTM standard, allowed reproducing on small scale severe heat exposure conditions. Hence, the experimental characterization of the PFP material was carried out by measuring the dynamic temperature evolution on a steel board covered by the tested product. The numerical model was applied to simulate several fire exposure conditions and insulating thickness, providing guidelines for PFP design and evaluating a specific Key Performance Indicator. Although several simplifications were introduced in the model, the present methodology may be used as a preliminary design tool, to be further integrated with real scale experiments and models.

References

American Society for Testing Materials (1994). ASTM E162-94 - Standard test method for surface flammability of materials using a radiant heat energy source, ASTM International, West Conshohocken.

Argenti F., Landucci G., 2013, Experimental and numerical methodology for the analysis of fireproofing materials, J. Loss Prev. in the Proc. Ind., in press, 1-12. DOI: 10.1016/j.jlp.2013.05.005

Birk A.M., 2005, Thermal Model Upgrade for the Analysis of Defective Thermal Protection Systems. Transportation Development Centre - Transport Canada, Ottawa, Canada.

Birk A.M., Poirier D., Davison C., 2006, On the response of 500 gal propane tanks to a 25% engulfing fire, J. Loss Prev. in the Proc. Ind.,19, 527–541.

Cotgreave T., 1992, Passive fire Protection: Performance Requirements and Test Methods, OTI Report 92606. SCI HSE, London.

Di Padova A., Tugnoli A., Cozzani V., Barbaresi T., Tallone F., 2011, Identification of fireproofing zones in Oil&Gas facilities by a risk-based procedure, J. Hazard. Mater. 191(1-3), 83-93.

Droste B., Schoen W., 1988, Full scale fire tests with unprotected and thermal insulated LPG storage tanks, J. Hazard. Mater. 20, 41-53.

Gomez-Mares M., Tugnoli A., Landucci G., Cozzani V., 2012a, Performance assessment of passive fire protection materials, Ind. and Eng. Chem. Res. 51, 7679–7689.

Gomez-Mares M., Tugnoli A., Landucci G., Barontini F., Cozzani, V., 2012b, Behavior of intumescent epoxy resins in fireproofing applications, J. of Analyt. and App. Pyrolysis, 97, 99–108.

Landucci G., Rossi F., Nicolella C., Zanelli S., 2009a, Design and testing of innovative materials for passive fire protection, Fire Saf. J. 44, 1103–1109.

Landucci G., Molag M., Cozzani, V., 2009b. Modeling the performance of coated LPG tanks engulfed in fires, J. Hazard. Mater. 172, 447–456.

Modest M.F., 2003, Radiative Heat Transfer, 2nd ed. Academic Press, New York.

Roberts A., Medonos S., Shirvill L. C., 2000, Review of the Response of Pressurized Process Vessels and Equipment to Fire Attack, Report OTO 2000 051, HSL, Manchester, UK.

Roberts T.A., Shirvill L.C., Waterton K., Buckland I., 2010, Fire resistance of passive fire protection coatings after long-term weathering, Proc. Saf. and Env. Prot. 88, 1-19.

Townsend W., Anderson C.E., Zook J., Cowgill G., 1974, Comparison of Thermally Coated and Uninsulated Rail Tank-Cars Filled with LPG Subjected to a Fire Environment, report FRA-OR&D 75-32, US Department of Transportation DOT, Washington, DC.

Tugnoli A., Cozzani V., Di Padova A., Barbaresi T. Tallone F., 2012, Mitigation of fire damage and escalation by fireproofing: A risk-based strategy, Rel. Eng. and Sys. Saf. 105, 25-35.

Tugnoli A., Cozzani V., Di Padova A., Barbaresi T., Tallone F., 2013, Reducing the consequences of accidental fires in oil&gas facilities: a risk-based procedure for identification of the fireproofing zones, Chemical Engineering Transactions, 32, 103-108, DOI:10.3303/CET1332018

Venart J.E.S., 1999, Boiling Liquid Expanding Vapor Explosions (BLEVE): possible failure mechanisms. ASTM Special Technical Publication, 1336, 112–134.

Wei G., Liu Y., Zhang X., Yu F., Du X., 2011, Thermal conductivities study on silica aerogel and its composite insulation materials, Int. J. of Heat and Mass Transf. 54, 2355-2366.